

A Simplified Method to Assess the Toppling Potential of Ground Motions: Application to Rocking–Isolated Frame Structures

F. Gelagoti, R. Kourkoulis

Soil Mechanics Laboratory, National Technical University, Athens, Greece

ABSTRACT: This paper aims to explore the limitations associated with the design of "*rocking–isolated*" frame structures. According to this novel seismic design concept the foundation is intentionally under-designed (so as to present lower moment capacity than the corresponding column), with the intention to bound the inertia loading that may be transmitted to the superstructure. Yet, decreasing footing dimensions increases the risk of toppling. Motivated by the need to address this issue in design, this paper proposes the peak spectral displacement of an earthquake record as a conservative upper-bound estimate of displacement demand. The adequacy of the measure is validated through comparison with published analytical and numerical results. Finally the paper attempts an investigation on the record characteristics affecting the overturning potential of ground motions, concluding that the impact pulse velocity and the number of cycles exceeding the toppling acceleration play prominent role.

1 INTRODUCTION

Recorded accelerations during strong earthquakes over the last 20 years very often overly exceeded code provisions: in the 1994 Northridge earthquake ($M_s = 6.8$) the maximum recorded P.G.A. exceeded 0.90 g; the 1995 Kobe earthquake ($M_s = 7.2$) produced maximum recorded acceleration of $a = 0.85$ g, while the 2007 Niigata-ken Oki earthquake produced an acceleration of $a = 1.20$ g. Such events have demonstrated that non-linear foundation response is indeed inevitable during strong seismic shaking. In fact, ensuring elastic foundation response may even be totally undesirable since enormous ductility demands would be imposed on the superstructure. On the other hand, allowing "plastic hinging", in the form of foundation uplift could be beneficial for the superstructure as it would bound the inertial forces transmitted to it [Psycharis and Jennings, 1983; Yim & Chopra, 1984; Martin & Lam, 2000; Pecker & Pender, 2000; Faccioli et al., 2001; Kutter et al., 2003; Harden and Hutchinson, 2006; Gajan and Kutter, 2008; Kawashima et al., 2007; Apostolou et al., 2007; Paolucci et al., 2008; Chatzigogos et al., 2009; Anastasopoulos et al, 2010].

The potential effectiveness of the mechanisms of foundation uplifting on frame structures has recently been investigated by Gelagoti et al (2011) for a simple 2-storey 1-bay frame (Fig. 1). Since foundation plastic "hinging" is mainly in the form of rocking and uplifting of the footing, the proposed design concept is termed *rocking isolation*, following the terminology proposed by [Mergos and Kawashima, 2005].

The authors compared the seismic performance of a conventionally designed structure (with square footings of $B = 1.7$ m) to a specific rocking-isolation alternative (with smaller footings of $B = 1.4$ m, Fig. 1). In this latter case footings were designed so that their moment capacity (M_{ult}) is smaller than that of the corresponding column. Hence, when the earthquake demand exceeds the footing capacity of the foundation, uplift is promoted. In all cases examined the Safety Fac-

tor against vertical loads was adequately high ($FS_v > 6$) so as foundation rocking prevails and soil yielding is impeded.

Through static pushover and nonlinear dynamic time-history analysis (using an ensemble of 24 strong motion records), the performance of the rocking-isolated alternative was found to be advantageous in very strong seismic shaking, well in excess of the design limits: it survives the earthquake demand sustaining non-negligible but repairable damage to its beams and non-structural elements (infill walls, etc.). Further decrease of foundation width (and subsequently further reduction of the foundation moment capacity) was shown to provide even more effective rocking isolation, yet at the expense of augmented foundation rotation or increased risk of frame toppling.

Motivated by the need to estimate a safe lower-bound dimension of rocking-isolated frame footings this paper aims to develop a simplified yet conservative procedure to estimate the maximum credible earthquake displacement demand (δ_{dem}). This demand may subsequently be combined with the (known) displacement capacity of the rocking superstructure to assess the minimum allowable footing dimensions that would ensure structural integrity of the superstructure.

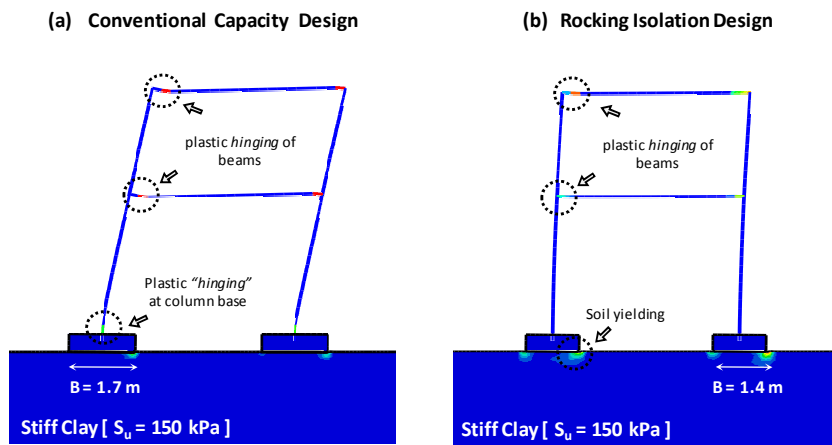


Figure 1: (a) Schematic illustration of the “rocking-isolation” concept that was thoroughly investigated at *Gelagoti et al (2010)*: Plastic Strains contours superimposed with deformed mesh when the two frames are excited by the extremely strong Takatori (Kobe, 1995) record. The conventionally designed frame collapses (plastic hinges are formed at the base of the two columns), while the rocking-isolation alternative survives despite the severity of the excitation.

Recalling that the apparent period of a rocking system changes constantly during shaking, rising from zero (in the case of a rigid block glued to its base) to infinity at the state of incipient toppling (Fig. 2), T_{eff} can neither be known a-priori nor can it be accurately estimated by means of conventional iterative procedure (Makris and Konstantinidis; 2003). Following this reasoning, in this research the peak spectral displacement SD_{max} is proposed as a conservative measure of the *upper bound* displacement demand (i.e. independent of T_{eff}). It is noted that SD_{max} is only proposed as an index of the maximum anticipated seismic displacement demand, knowing that this will not necessarily develop during shaking.

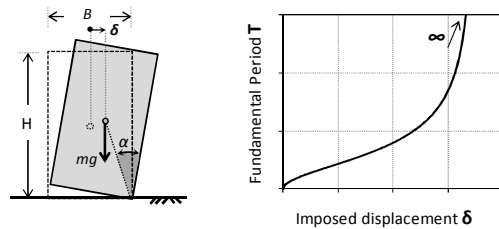


Figure 2. Evolution of the apparent natural period T with imposed displacement δ during rocking of a rigid block on rigid base. At the state of incipient toppling, T tends to infinity.

The validity and limitations of this simplified approximation are investigated in the following sections for two classes of rocking bodies: (i) a rigid-block on a rigid-base, and (ii) a nonlinear frame structure on inelastic soil.

2 VALIDATION OF THE APPROACH: RIGID BLOCK ON RIGID BASE

The issue of earthquake-induced rocking of *rigid blocks* on *rigid base* has been thoroughly investigated [Housner, 1963; Psycharis & Jennings, 1983; Koh et al., 1986; Makris & Roussos, 2000; Apostolou et al., 2007], and quite invariably it was demonstrated that overturning is rather unpredictable – *if not chaotic* – even for idealized cycloidal pulses as excitation. Hence, attempting to accurately quantify the toppling potential of a seismic motion (for a given *rigid block*) utilizing the simplified SD_{max} criterion would be overly optimistic and is by no means attempted herein. Instead, the present study aims to propose SD_{max} only as a *conservative upper-bound* of earthquake displacement demand δ_{dem} , for which toppling will not take place. The exploration presented in this paragraph refers to a rigid block on a rigid base subjected to (a) cycloidal (sinus and cosine) pulses, and (b) Ricker wavelets.

2.1 Rigid block excited by sinus and cosine pulses

A rigid block of width B and height H (Figure 2) is characterized by its angle $\alpha = \tan^{-1}(B/H)$ and the frequency parameter p :

$$p = \sqrt{3g/4R} \quad (1)$$

where $R = \sqrt{(\frac{B}{2})^2 + (\frac{H}{2})^2}$. The latter, which can be seen as a measure of the dynamic characteristics of the block, decreases with the size of the block. *Zhang & Makris [2001]* investigated analytically the transient rocking response of free-standing rigid blocks subjected to trigonometric (sine and cosine pulses) base excitation. Their rigorous analytical results are used herein as a comparison with the SD_{max} approach estimations. A relatively “small” block of $p = 2.14$ rad/s and $\alpha = 0.25$ rad is used as an illustrative example. The block is excited by one-cycle sinus (Fig. 3a) and cosine pulses (Fig. 3b) of amplitude a and cyclic frequency ω_p . The non-dimensional toppling acceleration $a_p/\alpha g$ is plotted as a function of normalized excitation frequency ω_p/p . The predictions of the simplified SD_{max} approach (distinct markers) are compared with the results of the exact analytical solution (shaded areas indicate toppling of the block).

It can be seen that both in the rigorous and the simplified approach, the non-dimensional toppling acceleration $a_p/\alpha g$ increases exponentially with ω_p/p ; this reveals that $a_p/\alpha g$ increases with excitation frequency *and* block dimensions ($1/p \propto \sqrt{R}$). In fact for the sinus pulse, the SD_{max} approach yields conservative results for the whole frequency range. However, for the cosine pulse, although conservative for lower and higher values of the frequency ratio ($\omega_p/p \leq 1.8$ and $\omega_p/p \geq 4.3$) it becomes marginally unconservative for intermediate frequencies ($1.8 < \omega_p/p < 4.3$). However this “unsafe region” is of reduced practical interest for relatively large systems such as low rise frames where p values normally range between $0.6 < p < 1$, and consequently the ratio ω_p/p is always greater than 4 for pulse periods $T_p < 1.6$ s (i.e., almost the complete earthquake period range).

2.2 Rigid block subjected to Ricker pulses

Gerolymos et al. (2005) based on dynamic time-history results, employed artificial neural networks to derive closed-form analytical expressions for predicting the overturning acceleration a_p of a rigid block subjected to Ricker pulses as a function of its geometric properties: Figure 4 depicts the comparison of the simplified SD_{max} - based prediction with the numerical solution of *Gerolymos et al. (2005)* for (i) a medium-size block of $p = 3.14$ rad/s and $\alpha = 0.25$ rad, simulating an *electrical transformer* ; and (ii) a large-size block of $p = 0.76$ rad/s and $\alpha = 0.30$ rad, simulating a *slender building*. Evidently, in accord with our previous observation, the larger the

dimensions of the rocking body, the greater the degree of conservatism of the SD_{max} -based method, whereas for very high frequency motions the simplified procedure underpredicts the toppling capacity by a factor greater than 1.5.

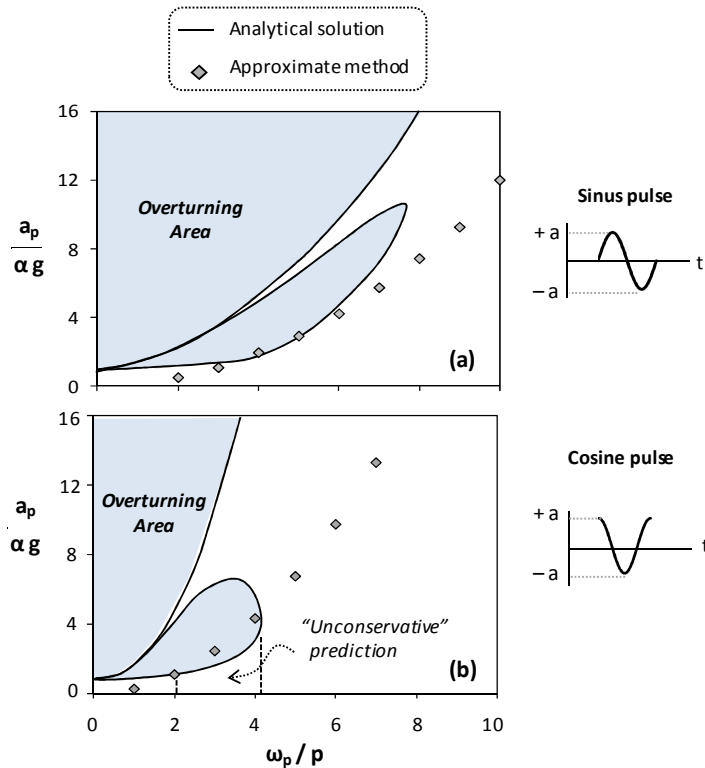


Figure 3. Non-dimensional toppling acceleration of a rigid body rocking on a rigid base: Comparison of the simplified method (based on the maximum spectral displacement SD_{max}) with the rigorous analytical solution of Zhang & Makris (2001) for two idealized excitation pulses: (a) one-cycle sinus, and (b) one-cycle cosine. Case study: rigid block of $p = 2.14$ rad/s and $\alpha = 0.25$ rad.

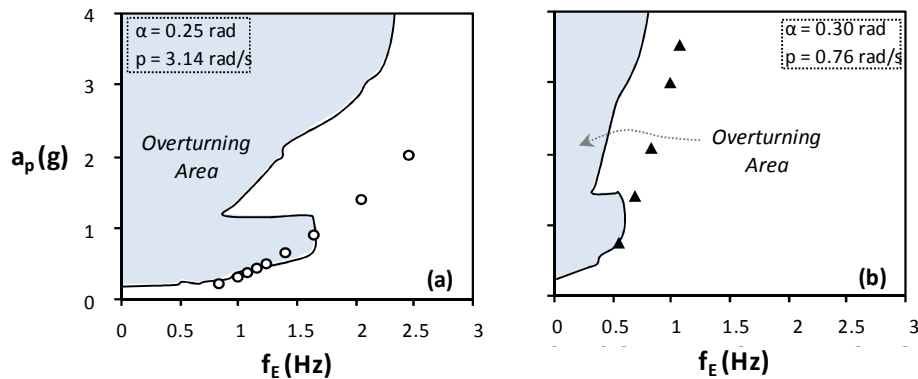


Figure 4. Toppling acceleration a_p of a rigid body rocking on a rigid base when excited by Ricker pulses of various f_E : Comparison of a_p estimated by the simplified method with the numerical solution of Gerylmos *et al.* [2005], plotted as a function of excitation frequency f_E for: (a) a medium-size block (electrical transformer) of $p = 3.14$ rad/s and $\alpha = 0.25$ rad, and (b) a large-size block (slender building) of $p = 0.76$ rad/s and $\alpha = 0.30$ rad

3 VALIDATION OF THE APPROACH: 2-STOREY FRAME ON INELASTIC SOIL

Having gained confidence on the results of the SD_{max} approach when implemented to estimate the toppling capacity of a rigid block on a rigid base, this section further verifies its effectiveness for the case of the 2-storey frame founded on nonlinear soil, subjected to both Ricker pulses and actual seismic records. To this end time history non-linear FE analyses had been conducted for the example frame (of Fig. 1) founded on footings of $B = 1.10$ m. Based on the $M-\theta$ response of the two footings (Fig. 5), the toppling rotation is $\theta_{ult} = 0.143$ rad, corresponding to a toppling displacement at the center of mass of the frame $\delta_{topl} = 71$ cm (ignoring frame's flexibility). Hence, according to the simplified approach, any motion with $SD_{max} < \delta_{topl}$ should not provoke toppling of the frame.

To validate this, the FE model have been subjected to amplitude-scaled excitations with SD_{max} marginally lower than the toppling displacement δ_{topl} of the frame (e.g., $SD^- = 0.9 \delta_{topl}$). In order to investigate the possible safety margins of the proposed methodology, the input motions are also scaled to $SD_{max} = 1.1 \delta_{topl}$ ($= 78$ cm), denoted SD^+ .

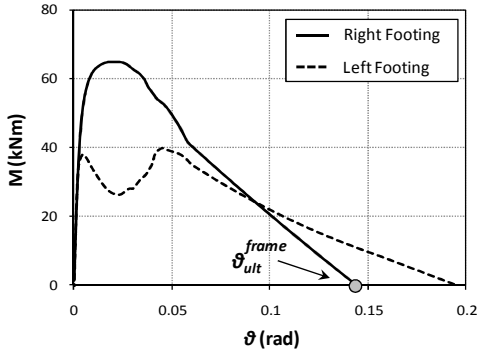


Figure 5. $M-\theta$ response of the two frame footings. [Results correspond to the frame of Figure 1 assuming foundation width of $B=1.1$ m]

3.1 Frame subjected to Ricker pulses

Ricker pulses of seven different characteristic frequencies, $f_E = 0.40, 0.50, 0.65, 0.85, 1.00, 1.25,$ and 1.50 Hz, have been used whose amplitude was sequentially increased until toppling of the frame. The minimum acceleration amplitude of each motion which provokes failure of the F.E. model is considered to be the “actual” (rigorously computed) toppling acceleration a_p . Fig. 6b, plots a_p as a function of normalized frequency ω_p/p of the system, and compares it to the predicted $(a_p)_{SD}$ toppling acceleration. Evidently, for all frequencies examined, the simplified approach yields a reasonably conservative prediction, while the margin of safety increases with increasing ω_p/p .

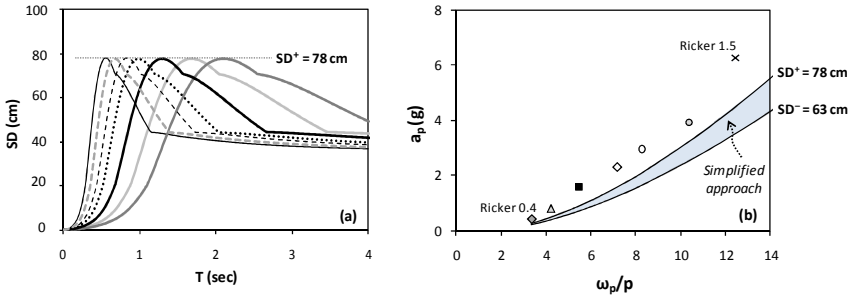


Figure 6. Comparison of simplified method with dynamic time history analysis of the frame on nonlinear soil subjected to Ricker pulses of various dominant frequencies f_E : (a) displacement response spectra SD of scaled Ricker pulses (to produce $max SD^+ = 78$ cm), (b) comparison of FE computed toppling acceleration a_p with the predicted $(a_p)_{SD}$ as a function of non-dimensional excitation frequency ω_p/p .

3.2 Real Records

18 recorded earthquake motions from the US, Europe, and Asia are utilized as excitation of the frame. The records were selected so as to enable us to capture the effects of various parameters, such as PGA and PGV, SA and SD, frequency content, duration, number of strong motion cycles. As previously, the validity of the SD_{\max} prediction is verified through dynamic nonlinear time-history analysis of the frame, where all input motions have been scaled at SD^+ (Fig. 7a) and SD^- values respectively. (Table 1). The produced Spectral Accelerations of the scaled accelerograms are displayed in Fig. 7b.

Quite encouragingly when the imposed displacement amplitude is SD^- – i.e a mere 10% lower than the toppling displacement ($SD^- = 0.9\delta_{ult}$) – toppling is avoided for all records. It is interesting to note that even for the SD^+ scaled seismic motions ($SD^+ = 1.1\delta_{ult}$), in most cases the frame will not topple. Yet, in only 2 (and admittedly highly amplified) of the records examined, the SD^+ scaled ground motion will produce overturning of the frame. Although this observation does not question the applicability of the simplified approach (since the imposed SD is 10% higher than the toppling displacement δ_{ult}) a more detailed insight into the factors affecting the toppling potential of a seismic excitation is attempted in the next section.

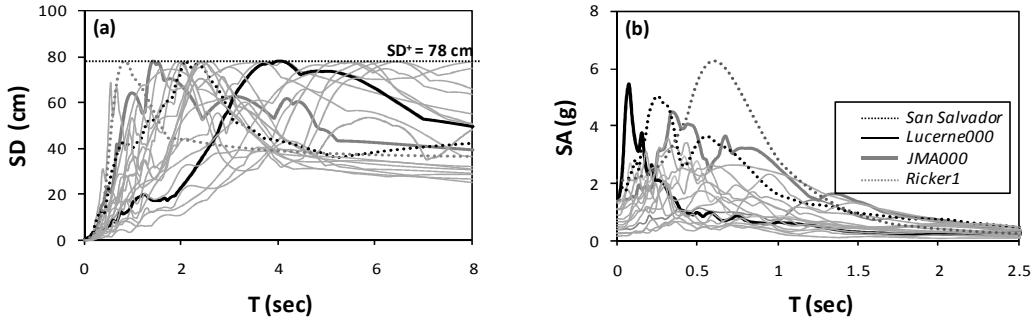


Figure 7: (a) displacement and (b) acceleration response spectra of actual acceleration time histories recorded during devastating earthquakes scaled *appropriately* to achieve $SD = 78$ cm. Four ground motions are distinguished and are further discussed.

4 INVESTIGATION OF THE TOPPLING POTENTIAL OF A GROUND MOTION

It is well known that a number of factors affect the toppling potential of a seismic motion [Makris & Roussos, 2000; Apostolou et al., 2007]. Aiming to better quantify it, a destructiveness measure is proposed herein, which is termed as the *cumulative impact pulse velocity* and is defined as:

$$V_{imp,max} = \max |V_{imp}| = \max \left| \int_0^{t_{tot}} (a - a_{yield}) dt \right| \quad (2)$$

where t_{tot} is the total duration of the ground motion, a the motion acceleration and a_{yield} is the minimum acceleration that when applied pseudostatically to the footing may provoke uplift. An approximate yet simple way to calculate a_{yield} is:

$$a_{yield} = \frac{(SA)_D M_{ult}^{footing}}{M_{RD}^C} \quad (3)$$

where $(SA)_D$ is the design spectral acceleration of the frame, $M_{ult}^{footing}$ is the overturning moment capacity of the footing, and M_{RD}^C is the bending strength of the corresponding column. The effect of the aforementioned measure on the toppling potential of ground motions is inves-

tigated in the sequel for the example frame with footing width $B = 1.1$ m. For this case $a_{yield} = 0.15 g$.

Figure 8 compares the Lucerne-000 record (Landers, 1992) with the GIC-090 record (San Salvador, 1986), both scaled to $SD^+ = 78$ cm. Although the Lucerne record contains a large number of peaks that exceed the yield acceleration a_{yield} (Fig. 8a), it does not contain a large impact velocity pulse $V_{imp,max}$ (Fig. 8b), and is therefore not leading to appreciable foundation rotation (Fig. 8c). In stark contrast the San Salvador record, despite boasting a considerably smaller number of strong motion cycles (and duration), is characterized by a substantially larger $V_{imp,max}$ (2.04 m/s compared to 0.78 m/s of Lucerne). Therefore it produces constant accumulation of rotation and eventually causes toppling of the structure. The time histories of V_{imp} reveal the key disparity between the two records. The effect of a clearly recognizable pulse produces a prominent "impact" on the structure, dragging it definitely beyond its equilibrium position. Depending on the amplitude of this *velocity impact pulse*, the increase of rotation following loss of equilibrium may bring about toppling of the structure. This effect is obvious on the time history of footing rotation θ for the San Salvador record: the large *impact velocity pulse* at $t = 1.4$ s produces a large rotation value $\theta \approx 0.08$ rad. Although this rotation alone is undeniably far lower than the toppling rotation $\theta_{ult} = 0.186$ rad, it causes an irrecoverable deviation from the initial equilibrium position while the subsequent strong motion cycles generate further accumulation of θ until, ultimately, toppling. The picture is significantly altered in case of the Lucerne record. Despite its multitude of strong motion cycles substantially exceeding a_{yield} , none of them boasts the kinematic characteristics (asymmetry *and* low frequency, i.e. large duration) to produce a large enough V_{imp} . As a result, the produced footing rotation θ fluctuates around zero, while the residual rotation remains relatively small.

The previous comparative example suggests that $V_{imp,max}$ may reveal certain characteristics of a seismic motion, mainly related to the existence of impact velocity pulses. However, it is still not adequate for the complete description of the toppling potential of a strong earthquake motion. For this purpose, the JMA-000 record (Kobe, 1995) is compared with a Ricker 1 pulse (i.e. $f_E = 1$ Hz). As shown in Fig. 9, the Ricker 1 pulse (scaled with respect to PGA) describes sufficiently the prevailing strong motion pulse of the JMA record.

In the context of the SD_{max} approach, the two ground motions are scaled to $SD^+ = 78$ cm. As shown in Fig. 9a, the Ricker 1 requires larger scaling ($PGA = 2.2 g$) to produce the same maximum spectral displacement with the JMA record (whose $PGA = 1.4 g$). Despite the fact that its *impact pulse velocity* $V_{imp,max} = 2.1$ m/s (Fig. 9b) is substantially larger than that of the scaled JMA record (of $V_{imp,max} = 1.87$ m/s), Ricker 1 is clearly inadequate to provoke toppling. The rotation $\theta \approx 0.09$ rad generated by the first pulse of Ricker 1 (Figure 9c) is recovered during the next (of opposite direction) cycle of motion. Due to the lack of subsequent strong motion pulses, the loss of equilibrium does culminate in toppling. On the other hand, the JMA record contains a prevailing strong motion cycle (at $t = 8$ s) which generates similar footing rotation θ as Ricker 1, however, its subsequent strong motion cycles which exceed a_{yield} produce gradual accumulation of θ ultimately resulting in toppling, which reveals that the number of cycles exceeding a_{yield} play an important role in the toppling potential of the ground motion.

4.1 The paradox of the Chi-Chi Record

The preceding discussion focused on the safety margin provided by the simplified SD_{max} approach, revealing that a *Factor of Safety* of the order of 1.1 may be considered adequate for real seismic motions. In reality, however, such *tremendous* seismic motions (e.g. the devastating JMA record scaled up at 1.4 g) have never been recorded and cannot possibly be considered realistic, especially for design purposes. This observation is of particular importance, since it implies that toppling can be quite *improbable* for real seismic motions, even in case of occurrence of *extremely strong earthquakes* (such as the ones deliberately selected for analysis), and even for *extremely under-designed* footings ($B = 1.1$ m).

Although the selected records cover a wide range of seismic motions, none of them is charac-

terized by fling-step effects — a different category of near-source effects, associated with large permanent displacement rather than a large velocity pulse. As shown in the examples of Figure 10a, such ground motions are characterized by excessively large spectral displacements. For example, the TCU-068 records (Chi-Chi, Taiwan 1999) yield SD_{max} of the order of several meters, i.e. almost an order of magnitude larger than δ_{ult} . With such large SD_{max} , it would be expected that the structure would easily be lead to toppling. To unravel the response of the system when subjected to this special category of near-source seismic motions, additional analyses are conducted utilizing the original records (without any scaling). Quite remarkably, even for the very extreme case of the TCU-068(NS) record (Fig. 10a), the footing experiences almost negligible rotation θ (Fig. 10b), and the structure is not toppling.

As paradox as this may appear, it is explainable on the basis of the acceleration time history. Despite the large SD_{max} , the yield acceleration a_{yield} is only slightly exceeded, and not for a long duration. This means that both V_{imp} and t_{yield} , and consequently TPi , are not large enough to provoke toppling. This implies that the long-period (almost quasi-static) component of the seismic motion, which is responsible for the excessive SD_{max} , is not really exceeding a_{yield} and, therefore, cannot lead to toppling. As clearly seen in Fig. 10a, the acceleration pulses that do exceed a_{yield} are of much higher frequency, and are not associated with the large SD_{max} of the record. This example reveals the notable conservatism of the simplified approach, for such special cases of near source seismic motions characterized by fling-step effects.

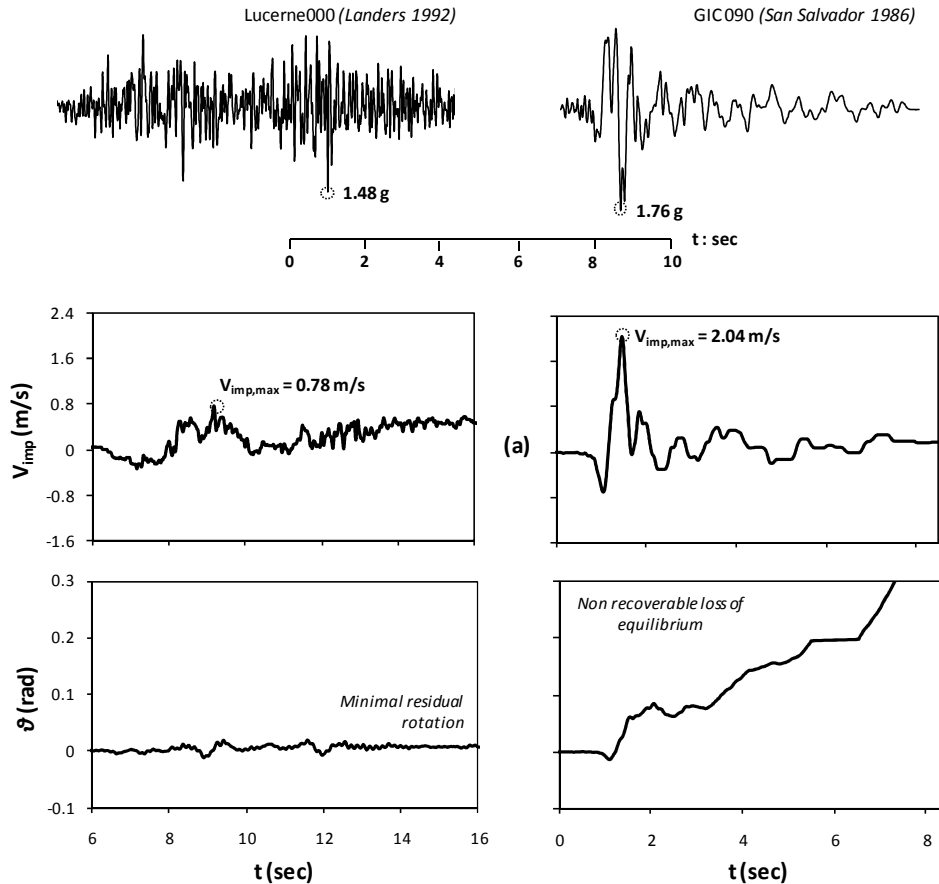


Figure 8. Nonlinear dynamic time history analysis — comparison of the effects of the Lucerne-000 (left column) with the GIC-090 (right column) record, both scaled to $SD^+ = 78$ cm : (a) time histories of “impact velocity” V_{imp} (bold black line), and (b) time histories of footing rotation θ .

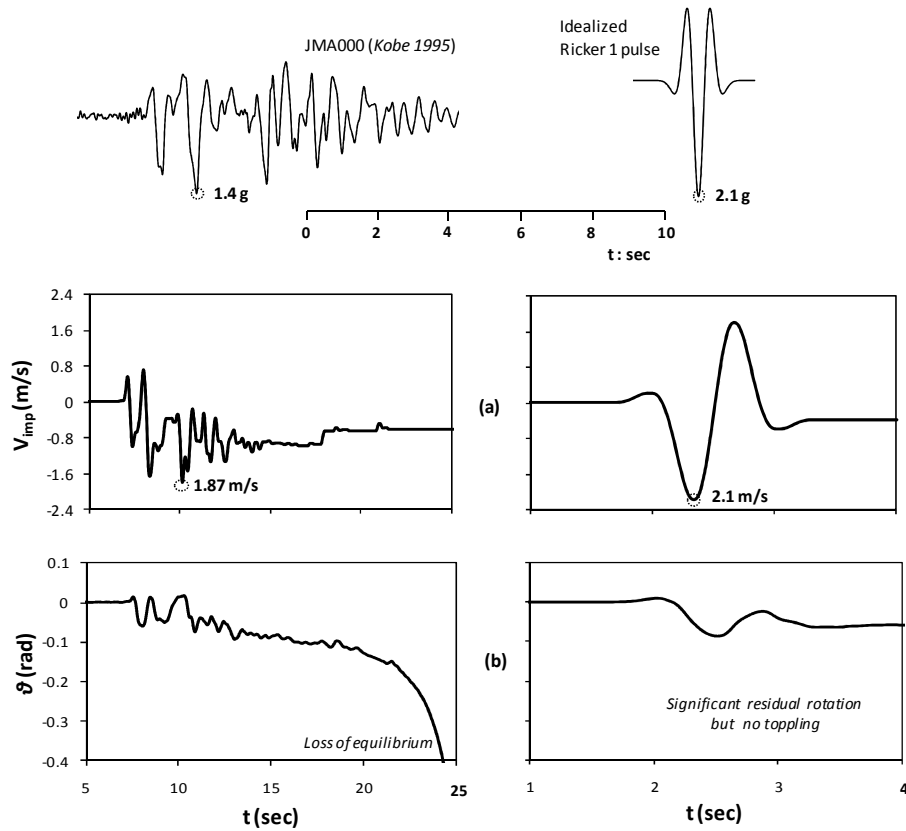


Figure 9. Nonlinear dynamic time history analysis – comparison of the effects of JMA-000 record with the Ricker 1 pulse both scaled to $SD^+ = 78$ cm : (a) time histories of “impact velocity” V_{imp} (bold black line) and (b) time histories of footing rotation θ .

5 ACKNOWLEDGEMENT

The financial support for this paper has been provided under the research project “DARE”, which is funded through the European Research Council’s (ERC) “IDEAS” Programme, in Support of Frontier Research–Advanced Grant, under contract/number ERC-2-9-AdG228254–DARE.

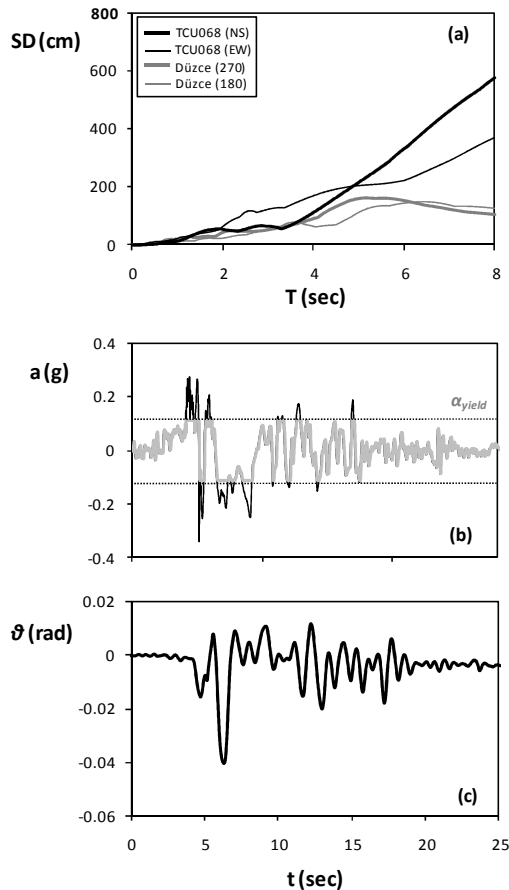


Figure 10. (a) Displacement response spectra of near-source motions characterized by fling-step effects. Nonlinear dynamic time history analysis of the frame subjected to seismic excitation with the TCU-068 (NS) record (Chi-Chi, Taiwan 1999) : (b) acceleration time history (the grey-shaded line represents the portion of the acceleration time history which lies below the yield acceleration α_{yield} – only a very small portion of the record exceeds α_{uplift} ; (c) time history of footing rotation θ .

6 REFERENCES

- ABAQUS, Inc. (2009), ABAQUS user's manual, Providence, R.I.
- Anastasopoulos I., Gazetas G., Loli M., Apostolou M, Gerolymos N. (2010), Soil Failure can be used for Earthquake Protection of Structures, *Bulletin of Earthquake Engineering*, 8, pp. 309–326.
- Anastasopoulos I. Gelagoti F., Kourkoulis R., Gazetas G. (2011) Simplified Constitutive Model for Simulation of Cyclic Response of Shallow Foundations : Validation against Laboratory Tests, *Journal of Geotechnical and Geoenvironmental Engineering*, ASCE (*in print*).
- Apostolou M., Gazetas G., Garini E. (2007), Seismic response of slender rigid structures with foundation uplifting, *Soil Dynamics and Earthquake Engineering*, 27 (7), pp. 642–654.
- Chatzigogos C.T., Pecker A., Salencon J. (2009), Macroelement modeling of shallow foundations, *Soil Dynamics and Earthquake Engineering*, Vol. 29, No. 6, pp. 765–781.
- Faccioli E, Paolucci R, Vivero G. Investigation of seismic soil– footing interaction by large scale cyclic tests and analytical models. *Proc. 4th International Conference on Recent Advances in Geotechnical Earthquake Engineering and Soil Dynamics*, Paper no. SPL-5, San Diego, California; 2001.

- Gajan S., Kutter B.L. (2008), Capacity, settlement, and energy dissipation of shallow footings subjected to rocking, *Journal of Geotechnical and Geoenvironmental Engineering*, ASCE, 134 (8), pp 1129-1141.
- Gelagoti F., Kourkoulis R., Anastasopoulos I., and G. Gazetas (2011), Rocking Isolation of Frames Founded on Isolated Footings, *Journal of Earthquake Engineering and Structural Dynamics* (*in print*)
- Gerolymos N., Apostolou M., Gazetas G. (2005), Neural network analysis of overturning response under near-fault type excitation, *Earthquake Engineering and Engineering Vibration*, 4 (2), pp. 213-228.
- Harden, C., Hutchinson, T. (2006), Investigation into the Effects of Foundation Uplift on Simplified Seismic Design Procedures, *Earthquake Spectra*, 22 (3), pp. 663–692.
- Housner G.W. (1963), The behavior of inverted pendulum structures during earthquakes. *Bulletin of the Seismological Society of America*, 53 (2), pp. 404–417.
- Kawashima K., Nagai T., Sakellarakis D. (2007), Rocking Seismic Isolation of Bridges Supported by Spread Foundations, *Proc. of 2nd Japan-Greece Workshop on Seismic Design, Observation, and Retrofit of Foundations*, April 3-4, Tokyo, Japan, pp. 254–265.
- Koh A.S., Spanos P., Roesset J.M. (1986), Harmonic rocking of rigid block on flexible foundation, *Journal of Engineering Mechanics*, ASCE, 112 (11), pp. 1165–1180.
- Kutter B.L., Martin G., Hutchinson T.C., Harden C., Gajan S., Phalen J.D. (2003), *Status report on study of modeling of nonlinear cyclic load–deformation behavior of shallow foundations*, University of California, Davis, PEER Workshop; March.
- Makris N., Konstantinidis D. (2003), The rocking spectrum and the limitations of practical design methodologies, *Earthquake Engineering & Structural Dynamics*, 32 (2), pp. 265–289.
- Makris, N., Roussos, Y. (2000), Rocking response of rigid blocks under near source ground motions, *Géotechnique*, 50 (3), pp. 243–262.
- Martin, G., R., and Lam, I. P. (2000). Earthquake Resistant Design of Foundations : Retrofit of Existing Foundations, *Proc. GeoEng 2000 Conference*, Melbourne.
- Paolucci R., Shirato M., Yilmaz M.T. (2008), Seismic behaviour of shallow foundations: Shaking table experiments vs numerical modelling, *Earthquake Engineering and Structural Dynamics*, Vol. 37, pp. 577–595.
- Pecker, A., & Pender, M.J., (2000), Earthquake Resistant Design of Foundations : New Construction, Invited paper, *GeoEng2000*, Vol 1, pp. 313-332.
- Psycharis I., Jennings P. (1983), Rocking of slender rigid bodies allowed to uplift. *Earthquake Engineering and Structural Dynamics*, 11, pp. 57–76.
- Yim C.S., Chopra A.K. (1984), “Earthquake response of structures with partial uplift on Winkler foundation”, *Earthquake Engineering and Structural Dynamics*, Vol. 12, pp. 263-281.
- Zhang J., Makris N. (2001), Rocking response of free-standing blocks under cycloidal pulses. *Journal of Engineering Mechanics*, ASCE, 127 (5), pp. 473–483.